ISSN 1063-7834, Physics of the Solid State, 2018, Vol. 60, No. 2, pp. 334–338. © Pleiades Publishing, Ltd., 2018.
Original Russian Text © A.D. Gorlov, 2018, published in Fizika Tverdogo Tela, 2018, Vol. 60, No. 2, pp. 329–332.

MECHANICAL PROPERTIES, PHYSICS OF STRENGTH, AND PLASTICITY

Effect of the Lattice and Spin–Phonon Contributions on the Temperature Behavior of the Ground State Splitting of Gd^{3+} in $SrMoO_4$

A. D. Gorlov

Institute of Natural Sciences and Mathematics of Ural Federal University, Yekaterinburg, Russia
e-mail: Anatoliy.Gorlov@urfu.ru

Received May 24, 2017

Abstract—The temperature behavior of the EPR spectra of the Gd^{3+} impurity center in single crystals of $SrMoO_4$ in the temperature range $T = 99–375$ K is studied. The analysis of the temperature dependences of the spin Hamiltonian $b_2^0(T) = b_2(F) + b_2(L)$ and $P_2^0(T) = P_2(F) + P_2(L)$ (for Gd^{157}) describing the EPR spectrum and contributing to the Gd^{3+} ground state splitting ΔE is carried out. In terms of the Newman model, the values of $b_2(L)$ and $P_2(L)$ depending on the thermal expansion of the static lattice are estimated; the $b_2(F)$ and $P_2(F)$ spin–phonon contributions determined by the lattice ion oscillations are separated. The analysis of $b_2^0(T)$ and $P_2^0(T)$ is evidence of the positive contribution of the spin–phonon interaction; the model of the local oscillations of the impurity cluster with close frequencies ω describes well the temperature behavior of $b_2(F)$ and $P_2(F)$.

DOI: 10.1134/S1063783418020117

1. INTRODUCTION

The molybdate compounds were and remain interesting materials for studying due to their application in practical devices. With their good optical properties and chemical inertness, they are used in different optoelectronic elements of various devices [1–3] and laser arrays [4]. With development of cryogen detecting technologies, the interest in molybdate compounds has grown; $CaMoO_4$ is the most used material for some devices. Being a scintillator in the X-ray band, $SrMoO_4$ demonstrates a higher efficiency than other molybdates; therefore, it can be used and is considered as a complimentary material [5]. Physical parameters of crystals determine the efficiency of devices and strongly depend on the phonon spectrum which changes with temperature (T). Theoretical models explaining such temperature changes related to the phonon spectra are still imperfect, so, new experimental results allowing one to separate the spin–phonon contribution (SPC) can help to develop them.

This work is a continuation of our EPR investigations [6, 7] devoted to the analysis of the change in the parameters of the initial splitting ΔE of the ground state of the Gd^{3+} impurity centers (IC) in crystals of $CaWO_4$ and $CaMoO_4$ due to the temperature changes in the ligand coordinates (implicit effect) and the effect of lattice oscillations, or the SPC (explicit effect) [8, 9]. We considered not only the greatest of the spin Hamiltonian (SH) parameters b_2^0 determining the splitting ΔE for $SrMoO_4$:Gd^{3+}, but also the quadrupole interaction (QI) P_2^0. It is known that the QI determined by the gradient of the electrical crystal field (CF) of ligands at the IC is proportional to the value of this field A_2^0 [10, 11]. Therefore, having separated the SPC from the values $b_2^0(T)$ and $P_2^0(T)$, we can expect that under the condition of a correct description of the spin–phonon interaction, some model parameters of these dependences must be identical.

2. EXPERIMENTAL RESULTS

A crystal of $SrMoO_4$:Gd^{3+} was grown by the Czochralski method with the Gd_2O_3 impurity of 0.02% by weight (with a natural content of isotopes) in the charge. The EPR spectra were recorded by the Bruker EMX plus spectrometer in the 3-cm band at different T and orientations of the external magnetic field $\mathbf{H}$. The permitted hyperfine structure (PHS) arising due to the Gd^{157} odd isotope (electron spin $S = 7/2$, nuclear spin $I = 3/2$) was observed for all EPR signals in the case of the $\mathbf{H} \parallel \mathbf{S}_4$ orientation of the principal crystallographic axis and for a few EPR signals in the case of $\mathbf{H} \perp \mathbf{S}_4$.

Table 1. Experimental parameters of the spin Hamiltonian of the Gd^{157} impurity ion in $SrMoO_4$ and the calculated lattice contribution of the static lattice to $Z_2(L)$ (in MHz) at different T

T, K	SH parameters				Calculated contribution of the static lattice	
	b_2^0	b_4^0	b_4^4	P_2^0	$b_2(L)$	$P_2(L)$
99	−2496.0(3)	−39.29(15)	−249.3(20)	−57.3(4)	−2519.7	−58.3
111	−2492.7(3)	−39.10(15)	−248.0(31)	−57.3(4)	−2523.1	−58.5
125	−2489.4(4)	−39.09(30)	−247.3(23)	−57.2(5)	−2527.4	−58.7
150	−2482.0(3)	−38.84(30)	−247.7(10)	−57.2(4)	−2536.1	−59.2
175	−2472.7(3)	−38.55(29)	−246.5(11)	−57.0(4)	−2545.9	−59.7
200	−2463.3(4)	−38.18(33)	−243.5(12)	−56.9(5)	−2556.8	−60.3
250	−2443.0(3)	−37.73(3)	−238.7(20)	−56.7(4)	−2581.2	−61.7
273	−2434.4(4)	−37.40(23)	−237.1(18)	−56.4(5)	−2593.5	−62.4
298	−2427.3(4)	−37.20(22)	−235.6(20)	−56.3(4)	−2605.7	−63.2
375	−2394.5(9)	−36.2(5)	−230.0(12)	−55.9(6)	−2653.5	−65.7

$g_x = g_y = 1.9915(4)$, $g_z = 1.9918(3)$, $b_6^0 = 0.16(10)$, $b_6^4 = 6(8)$, $b_6^6 = 2(6)$, $A_x = A_y = 16.2(3)$, $A_z = 16.2(3)$. The mean error in $b_2(L)$ due to the lattice parameter inaccuracy ~0.8% (~20 MHz); in $P_2(L)$, ~2.2% (~1.3 MHz).

The EPR spectrum from the even isotopes and an odd isotope is well described by the spin Hamiltonian corresponding to the D_{2d} local symmetry of IC, i.e., Gd^{3+} replaces Sr^{2+} [12]. The numerical minimization of the roof-mean-square deviation of the experimental and calculated signal positions has shown that the values of parameters $b_n^m(T)$ ($n = 2, 4, 6$ and $m = 0, 4, 6$) for the even isotopes and an odd isotope of Gd^{3+} in $SrMoO_4$ nearly coincide within the measurement error limits; the root-mean-square errors are also similar. The use of the SH for a real local IC symmetry S_4 did not lead to the reduction of errors in determining the parameters. Table 1 presents their values for Gd^{157} in $SrMoO_4$.

3. MODEL CALCULATIONS

Let us find $Z_n^m(T) = b_n^m(T)$ (or $P_n^0(T)$) as experimentally determined constants of the SH and the SPC to the diagonal parameters ($m = 0$) $Z_n(F) = b_n(F)$ (or $P_n(F)$). Then [6, 7]

$$Z_n(F) = Z_n^0(T) - Z_n(L). \quad (1)$$

For $n = 2$, $Z_2(L) = b_2(L)$ (or $P_2(L)$) are the static lattice contributions at a given T. Let us calculate the values of $Z_2(L)$ at different T with the help of the Newman superposition model [13–15] in the form presented in [16].

3.1. Calculation of the Lattice Parameters

To determine $b_2(L)$ and $P_2(L)$, it is necessary to know a and c lattice parameters for $SrMoO_4$ for a wide range of T. There are no such data for low temperatures in literature, however, the experimentally measured parameters a and c for $SrMoO_4$ for a temperature range $T = 299$–931 K are provided in [17]. We suggested that the dependences $a(T)$ and $c(T)$ have a polynomial form as in [18] ((6) for $CaWO_4$)

$$l(T) = l_0(1 + l_1T^2 + l_2T^3 + l_3T^4), \quad (2)$$

where $l = a$ or c. Using the data of [17] as reference points in the fitting procedure and (2), we obtained dependences $a(T)$ and $c(T)$ with parameters (in Å):

$$a_0 = 5.3888(16), \quad a_1 = 2.0438(199) \times 10^{-8},$$

$$a_2 = -2.045(245) \times 10^{-11}, \quad a_3 = 8.6(28) \times 10^{-15},$$

$$c_0 = 11.9861(48), \quad c_1 = 4.6014(836) \times 10^{-8},$$

$$c_2 = -4.565(110) \times 10^{-11}, \quad c_3 = 1.85(12) \times 10^{-14}.$$

The presented errors (the numbers in brackets) correspond to the tripled root-mean-square deviation 3σ. To verify the reliability of application of (2), we used a similar algorithm for the data of [19] for $CaMoO_4$ taken in a temperature range $T \sim 300$–1273 K. The obtained $a(T)$ and $c(T)$ show a satisfactory agreement with the experimental results of [20] in the range $T =$ 10–300 K. Using (2) with the above-determined a_i and c_i, we calculated the lattice parameters of $SrMoO_4$ at required T. After that, we calculated the spherical coordinates R, θ, and φ of the 8 oxygen ions (O^{2-}) nearest to Gd^{3+} in a pure $SrMoO_4$ lattice. The coordinates x, y, and z of these O^{2-} ions are taken from the data of [21].

3.2. Estimation of Parameters $Z_2(L)$

The algorithm of calculation of parameters $Z_2(L)$ in the superposition model [13–16] is similar to that described in [6, 7]. In the expression

$$Z_2(L) = \Sigma_i k_i(\theta)[Z_{2p}(R_0/R_i)^3 + Z_{2s}(R_0/R_i)^{10}] \quad (3)$$

the "intrinsic" parameters Z_{2p} ($b_{2p} = -1.289 \times 10^4$ MHz or $P_{2p} = -545.6$ MHz [16] are the contributions of a point charge O^{2-}. The coordination factors $k_i(\theta) = n(3\cos^2\theta_i - 1)/2$. Since the oxygens adjacent to Gd^{3+} are divided into two groups of four, equivalent in their contributions to b_2^0 and P_2^0, then $i = 1, 2$ and $n = 4$. The Gd^{3+}–O^{2-} distance is calculated according to the formula $R_i = R + (r - r_h)/2$ [22], where r and r_h are the ion radii of the impurity and replaceable ions, respectively, taken from the Shannon tables [23]. The parameters Z_{2s} ($b_{2s} = 1.008 \times 10^4$ MHz and $P_{2s} = 555.8$ MHz), i.e., the overlapping and covalence contributions at a distance $R_0 = 2.34$ Å [16], are determined for Gd^{3+} in $SrMoO_4$ as follows. From the dependences of experimental quantities $b_2^0(T)$ and $P_2^0(T)$ in the "hard lattice" model, according to (2)–(4) from [24], the values $Z_2^0(RL)$ were obtained. As it was shown in [6, 7], the values $Z_2^0(RL) = b_2^0(0)$ or $P_2^0(0)$ (further $Z_2^0(RL) = Z_2^0(0)$); i.e., they are close to the values of experimental parameters at $T \sim 1.8$–4.2 K, since the phonon contribution in this range of T is very small [6–9, 25–27]. It should be noted also that these values are obtained as nearly identical when using any parametrization model described in [24–27]. Having determined a and c at $T \sim 2$ K according to (2) and then R_i, θ_i, and φ_i for the Gd^{3+}–$8O^{2-}$ cluster and, using (3), one can easily obtain b_{2s} and P_{2s}. Table 1 presents the calculated values of $b_2(L)$ and $P_2(L)$ at required temperatures; Table 2, the parameters $b_2^0(0)$ and $P_2^0(0)$.

4. TEMPERATURE DEPENDENCE OF $Z_2(F)$ AND DISCUSSION OF RESULTS

Let us separate from our experimental data the temperature dependence for $b_2(F)$ and $P_2(F)$ which will be determined from (1) and the data of Table 1. It is seen that $b_2(F)$ and $P_2(F)$ are positive. One can try to use three most known theoretical models [25—27] to describe the SPC, depending on the temperature and influencing on the initial splitting of the energy levels ΔE for the IC in crystals. These models suggest the dominant contribution of the optical [25] or acoustical [26] phonons in the SPC. It is shown in the model of [27] that the main role in the phonon-induced contribution (or in the SPC) is played by the local optical oscillations of the impurity cluster. Despite the fact that each model gives a particular functional temperature dependence for $Z_2(F)$, they all give nearly linear dependence on T in the region $T > 200$ K.

Table 2. Model parameters of the temperature dependences $Z_n^m(T)$ and $Z_2(F)$ (in MHz) for Gd^{3+} in $SrMoO_4$

Dependences	Model parameters		
	$Z_n^m(0)$	$Z_n(0)$	$\omega \times 10^{-13}$, rad/s
$b_2^0(T)$	−2506.1(20)	50.0(18)	3.15(10)
$P_2^0(T)$	−57.4(46)	1.65(48)	5.58(87)
$b_4^0(T)$	−39.6(8)	1.3(1)	2.73(13)
$b_4^4(T)$	−250(5)	16.3(51)	4.6(8)
$b_2(F)$	–	126.8(96)	3.4(2)
$P_2(F)$	–	4.9(5)	3.47(50)

Errors in parameters correspond to 3σ.

4.1. Temperature Dependence of $b_2(F)$

The analysis has shown that in the models of [25, 26], the dependence of the phonon-induced contribution $b_2(F)$ on T can be described only by three fitting parameters, one of which does not have a theoretical justification. On the other hand, the local oscillation model [27] with two parameters describes very well the dependence of $b_2(F)$ on T by the expression

$$Z_2(F) = Z_2(0)[\coth(\omega/2kT) - 1], \quad (4)$$

where $Z_2(0) = b_2(0)$ is the contribution owing to the lattice "zero oscillations," ω is the frequency of local oscillations of the impurity cluster, and k is the Boltzmann constant. Figure 1 shows the dependence of $b_2(F)$ on T (curve *1*) obtained by using the genfit algorithm. The points on the curve are determined according to (1). Table 2 presents the model parameters; their deviations at 3σ are shown in brackets.

4.2. Temperature Dependence of $P_2(F)$

Despite the smallness of the changes in $P_2^0(T)$, the result of calculations of $P_2(L)$ shows that the phonon-induced contribution $P_2(F) \sim 7$ MHz at $T \sim 300$ K. Like in the case of $b_2(F)$, the models in [25, 26] require three fitting parameters in the genfit algorithm to express the temperature dependence of $P_2(F)$; the local oscillation model [27] well describes $P_2(F)$, according to (4) (curve *2* in Fig.1). The model parameters are shown in Table 2; the presented errors are determined also at 3σ.

The ratio of the changes in the lattice contribution $\Delta b_2(L) = |b_2(L) - b_2^0(0)|$ to $|b_2(F)| \sim 0.56$ at $T = 298$ K;

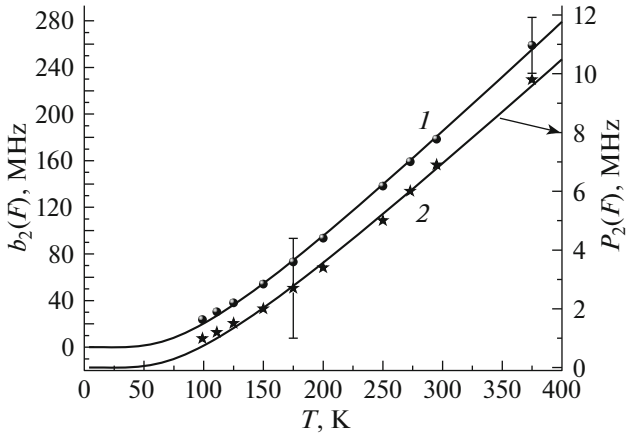

Fig. 1. Temperature dependences of $b_2(F)$ (*1*), $P_2(F)$ (*2*). Curves *1* and *2* are described by expression (4) with parameters presented in Table 2. The positions of dots and asterisks are determined according to (1) and (3). The presented errors include the maximum experimental error in $b_2^0(T)$ and $P_2^0(T)$ and the spread in $b_2(L)$ and $P_2(L)$ due to the inaccuracy in calculating the lattice parameters.

$\Delta b_2(L) < 0$. It means that the contribution of the local oscillations of the impurity cluster centers to the temperature change in $b_2^0(T)$ is 1.7 times as much as the change in $\Delta b_2(L)$ due to the static lattice expansion. Similar estimations for the QI give $\Delta P_2(L) = P_2(L) - P_2^0(0) < 0$ and $|\Delta P_2(L)/P_2(F)| \sim 0.8$, which means also a stronger influence of local oscillations on the temperature dependence of the QI. Since these two (phonon-induced and lattice) mechanisms make the contributions of opposite signs to $Z_2^0(T)$; they partly compensate each other, which can be especially noticed in the values $P_2^0(T)$.

Thus, we see that the positive values of the SPC $b_2(F)$ and $P_2(F)$ are described by (4) with frequencies ω that coincide within the error limits. Proceeding from this result, we consider that a unique description of the temperature dependences for the above-mentioned parameters justifies the use of the Pfister's model [27] that suggests the dominant role of the local oscillations of the impurity cluster in the phonon-induced contribution. It should be noted that a considerable effect of the local oscillations on the processes of the energy dissipation from the IC to the lattice is also observed in the optical range, which influences on the efficiency of operation of different devices used in practice (see [28] and references in it).

4.3. Temperature Dependence of b_n^m

The parameters $b_4^m(T)$ ($m = 0, 4$) were analyzed only in the "hard lattice model" [24], since there is no a satisfactory model to determine b_n^m and the use of the Newman's model [13–15] for their calculation gives ambiguous results, as it was shown earlier in [7]. Having taken (2), (3), and (4) from [24] for three SPC models, we obtained the values $b_4^m(RL)$ whose mean values are presented in Table 2.

5. CONCLUSIONS

The analysis of the experimental dependences of the SH parameters $b_2^0(T)$ and $P_2^0(T)$ for the Gd^{3+} impurity center (an odd isotope) in $SrMoO_4$ has shown that the consideration of the temperature changes in the static lattice contribution $\Delta Z_2(L) < 0$ made it possible to describe the temperature behavior of the spin–phonon interaction $b_2(F)$ and $P_2(F) > 0$ uniquely and with a minimum number of model parameters. The Pfister's model of local oscillations of the impurity cluster [27] proved to be the most appropriate among three SPC models; the frequencies of the local oscillations for $b_2(F)$ and $P_2(F)$ coincide with each other (within error limits). The ratio of the spin–phonon contribution to the temperature changes in the lattice contribution is ~1.7 in the region of the linear dependence for $b_2^0(T)$ and ~1.25 for $P_2^0(T)$. This shows that the initial splitting of the impurity cluster oscillations more strongly affects the temperature behavior than the lattice expansion. Since these contributions have opposite signs, they partly compensate each other in a wide temperature range, which considerably weakens the dependence $Z_2^0(T)$. It should be also noted that these results are similar to those obtained for Gd^{3+} in $CaMoO_4$ and $CaWO_4$.

ACKNOWLEDGMENTS

This work is carried out in the framework of the government task of the Ministry of Education and Science of Russia for the Ural Federal University (project no. 3.6115.2017/8.9) with the use of the equipment provided by the "Modern Nano-technologies' Multiaccess Center of the Ural Federal University.

REFERENCES

1. L.-Y. Zhou, J.-S. Wei, F.-Z. Gong, J.-L. Huang, and L.-H. Yi, J. Solid State Chem. **181**, 1337 (2008).
2. A. Khanna and P. S. Dutta, J. Solid State Chem. **198**, 93 (2013).
3. A. S. Shcherbakov, A. O. Arellanes, and S. A. Nemov, Opt. Eng. **52**, 064001 (2013).
4. V. Osiko and I. Shcherbakov, Fotonika **39**, 14 (2013).
5. H. Bhang, R. S. Boiko, D. M. Chernyak, J. H. Choi, S. Choi, F. A. Danevich, K. V. Efendiev, C. Enss, A. Fleischmann, A. M. Gangapshev, L. Gastaldo, A. M. Gezhaev, Y. S. Hwang, H. Jiang, W. G. Kang, et al., J. Phys.: Conf. Ser. **375**, 042023 (2012).

6. A. D. Gorlov, Phys. Solid State **57**, 1394 (2015).
7. A. D. Gorlov, Phys. Solid State **59**, 578 (2017).
8. W. M. Walsh, Jr., Phys. Rev. **114**, 1473 (1959).
9. W. M. Walsh, Jr., J. Jeener, and N. Bloembergen, Phys. Rev. A **139**, 1338 (1965).
10. A. Abragam and B. Bleaney, *Electron Paramagnetic Resonance of Transition Ions* (Clarendon, Oxford, 1970), vol. 1.
11. B. Bleaney, in *Hyperfine Interactions,* Ed. by A. J. Freeman and R. B. Frankel (Academic, New York, 1967), p. 1.
12. S. A. Altshuler and B. M. Kozyrev, *Electron Paramagnetic Resonance of Compounds of Elements of Intermediate Groups* (Nauka, Moscow, 1972), p. 429 [in Russian].
13. D. J. Newman and W. Urban, Adv. Phys. **24**, 793 (1975).
14. G. G. Siu and D. J. Newman, J. Phys. C **15**, 6753 (1982).
15. D. J. Newman, J. Phys. C **8**, 1862 (1975).
16. L. I. Levin and A. D. Gorlov, J. Phys.: Condens. Matter **4**, 1981 (1992).
17. V. T. Deshpande and S. V. Suryanarayana, Acta Crystallogr. A **28**, 94 (1972).
18. A. Senyshyn, H. Kraus, V. B. Mikhailik, and V. Yakovyna, Phys. Rev. B **70**, 214306 (2004).
19. S. N. Achary, S. J. Patwe, M. D. Mathews, and A. K. Tyagi, J. Phys. Chem. Solids **67**, 774 (2006).
20. A. Senyshyn, H. Kraus, V. B. Mikhailik, L. Vasylechko, and M. Knapp, Phys. Rev. B **73**, 014104 (2006).
21. E. Gurmen, E. Daniels, and J. S. King, J. Phys. Chem. Phys. **55**, 1093 (1971).
22. W. C. Zheng and S. Y. Wu, Physica B **304**, 137 (2001).
23. R. D. Shennon, Acta Crystallogr. A **32**, 751 (1976).
24. T. Rewajt, J. Kuriata, J. Typek, and J. Y. Buzare, Acta Phys. Polon. A **84**, 1143 (1993).
25. C. Y. Huang, Phys. Rev. **159**, 683 (1967).
26. K. N. Shrivastava, Phys. Rev. **187**, 446 (1969).
27. G. Pfister, W. Draybrodt, and W. Assmus, Phys. Status Solidi B **36**, 351 (1969).
28. M. P. Hehlen, A. Kuditcher, S. C. Rand, and M. A. Tischler, J. Chem. Phys. **107**, 4886 (1997).

Translated by E. Smirnova